5-2015

Surface Microstructure Evolution of Metallic Specimens Using the Large Chamber Scanning Electron Microscope

Grace Egbujor
Western Kentucky University, grace.egbujor279@topper.wku.edu

SURFACE MICROSTRUCTURE EVOLUTION OF METALLIC SPECIMENS USING THE LARGE CHAMBER SCANNING ELECTRON MICROSCOPE

A Thesis
Presented to
The Faculty of the Department of Physics and Astronomy
Western Kentucky University
Bowling Green, Kentucky

In Partial Fulfillment
of the Requirements for the Degree
Master of Science

By
Grace Egbujor

May 2015

SURFACE MICROSTRUCTURE EVOLUTION OF METALLIC SPECIMENS USING THE LARGE CHAMBER SCANNING ELECTRON MICROSCOPE

Date Recommended 4/17/15

Edward Kintzel, Director of Thesis

Keith Andrew

Ivan Novikov

4-20-15

Dean, Graduate Studies and Research Date

I dedicate this thesis to my parents Grace and Theo Egbujor for always praying for me. My family Uche, Chika, Ogechi, Raven, Theo Jr., and Michelle for always supporting me. My friends for always encouraging me!

ACKNOWLEDGMENTS

I would like to acknowledge Western Kentucky University especially the Nondestructive Analysis Center and Engineering and Biological Science building at Western Kentucky University for allowing me to conduct my research. I am acknowledging Dr. Keith Andrew and Ivan Novikov for being a part of my thesis committee. Dr. Christopher Byrne and Saxon Steele for helping me conduct tensile testing and helping me better understand stainless steel. Dr. Wieb Vandermeer and Phillip Womble for always supporting me! Finally, I would like to acknowledge Dr. Edward Kintzel for being my research advisor and helping me make it to the finish line.

CONTENTS

LIST OF FIGURES

LIST OF TABLES

SURFACE MICROSTRUCTURE EVOLUTION OF METALLIC SPECIMENS USING THE LARGE CHAMBER SCANNING ELECTRON MICROSCOPE

Grace Egbujor May 2015 39 Pages

Directed by: Edward Kintzel, Keith Andrew, and Ivan Novikov

Department of Physics and Astronomy Western Kentucky University

An initial study into the use of the large chamber scanning electron microscope (LC-SEM) to interrogate the surface microstructure evolution of metallic specimens has been carried out. The LC-SEM located at Western Kentucky University is the largest instrument of its type at any university in the world. As such, unique measurements can be performed due to the size of its chamber and extended view of its optic system. Strain was varied for each individual specimen, and imaged using Secondary Electrons within the gauge length as well as near the grip position. Results will show progression of surface microstructures and nickel content of metallic specimens. Additionally, results will demonstrate the capability of the LC-SEM to carry out these types of measurements. Future measurements will include the incorporation of an in-situ uniaxial load frame for dynamic studies.

INTRODUCTION

Section 1.1 History of Stainless Steel

Iron and steel making techniques can be traced back for thousands of years. Various dynasties, kingdoms, and colonies used steel making techniques; initially to create stronger weapons then for more commercial uses like cutlery. In comparison to the history of steel, stainless steel is a relatively new phenomenon only dating back 150 years. Various scientist, inventors, and metallurgists from all over the world have been credited for inventing stainless steel but the most credited metallurgist is Harry Brearley. He discovered stainless steel by accident while researching ways to eliminate erosion in gun barrels. (1) While the origin of stainless steel is still disputed; the impact of the stainless steel in technology is not. (2)

Stainless steel is praised for its abundant practical uses, making appearances in the architectural, commercial, automotive, medical, military, and industrial applications of manufacturing. It contains a high resistance to corrosion making it low maintenance. Its ability to withstand high magnitudes of temperature in both directions, high pressure, and still be malleable and ductile makes stainless steel the ideal material for manufacturing lasting, highly used products.

But what is stainless steel? Stainless steel is a generic term for a family of corrosion resistant alloy steels containing 10.5% or more chromium. Stainless steel is identified by three types: martenistic, ferritic, and austenitic and has over 150 grades of stainless steel.

1.2 Motivation

As mentioned above, stainless steel is used for many applications. Depending on the application, specific stainless steel grades are required. The stainless steel grade is used to classify stainless steel by their composition and physical properties (3). The most popular grade is the 300 series. Although the each stainless steel grade of the 300 series has different compositions of alloy steel; there are common factors that define the 300 series, such as carbon content, that is generally held to a maximum of 0.08%. They typically have 18% chromium, 8% nickel, and are non-magnetic. They cannot be hardened by heat treatment, and they can be hardened by cold working the material ("work hardening."). (4)

These combined composition and physical properties contribute to the reason the 300 series is the most popular grade. Of all the 300 series, type 304 and type 316 are the most prevalent used worldwide. (4) Specifically, in aspects of Homeland Security, type 304 and type 316 is being used in infrastructure, weaponry, military equipment, medical equipment, and a plethora of other things. When stainless steel failures occur for any of the items listed above, catastrophies can occur resulting in fatalities. A more detailed understanding of the fatigue behavior, deformation characteristics, and resulting microstructure changes of types 304 and 316 after undergoing strain is fundamentally important for current an new applications of this significant material.

MATERIALS AND METHODS

2.1 Materials

Stainless steel type 304 and type 316 were used as the testing material to investigate stainless fatigue behavior. Type 304 stainless steel, a Chromium-Nickel austenitic alloy, has a minimum of 18% chromium, 8% nickel, and a maximum of 0.08% carbon. Type 316 stainless steel is a molybdenum bearing stainless steel that contains 2% molybdenum, a minimum of 18% chromium, and minimum of 14% nickel.

Type 304 and Type 316 were selected because of their widespread use for a variety of military applications and power plant manufacturing. As well, the two types have a discernable nickel content. Nickel is a silvery-white metal that is primarily used to make stainless steel and other alloys stronger and better able to withstand extreme of temperature and resistance to corrosive environments. Approximately 80 percent of the primary (not recycled) nickel consumed in the United States in 2011 was used in alloys, such as stainless steel and super-alloys. Because nickel increases an alloy's resistance to corrosion and its ability to withstand extreme temperatures, equipment and parts made of nickel-bearing alloys are often used in harsh environments, such as those in chemical plants, petroleum refineries, jet engines, power generation facilities, and offshore installations.(5)

Section 2.2 Equipment

The equipment utilized during this investigation was: LECO AP-60 Polisher/Grinder, Instron by Satec Systems, Partners software, and the large chamber scanning electron microscope.

2.2.1 Polishing

A LECO AP-60 was used to polish all stainless steel dog bones. An AP-60 is an automatic polisher and grinder used for to help with microstructure analysis of metallurgic samples. In addition to using the AP-60, 180 grit silicon carbide grinding paper, 320 grit silicon carbide grinding paper, and 600 grit silicon carbide grinding paper, 6 micron diamond compound paste, 1 micron diamond compound paste, polish extender, ultra-fine silk polishing cloth, and red felt cloth were also used for polishing. All products used for polished were manufactured by LECO Corporation.

Figure 1: Leco AP-60 Grinder/Polisher

2.2.2 Tensile Testing

The Instron by Satec Systems Static Hydraulic Test Systems was used to conduct the tensile testing.

a.) 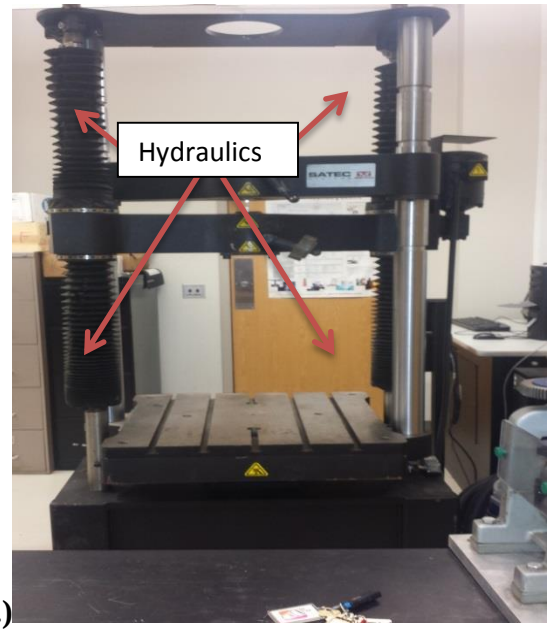

b.) 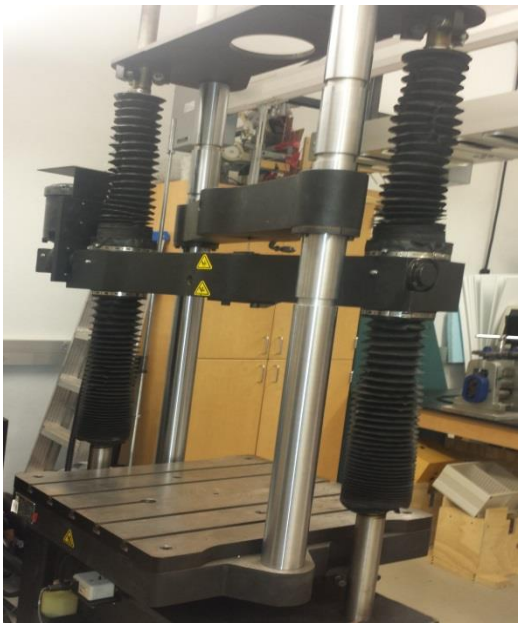

Figures 2: a-b Instron by Satec Systems

2.2.3 Data Acquisition

Partner software is the program used for data acquisition during tensile testing.

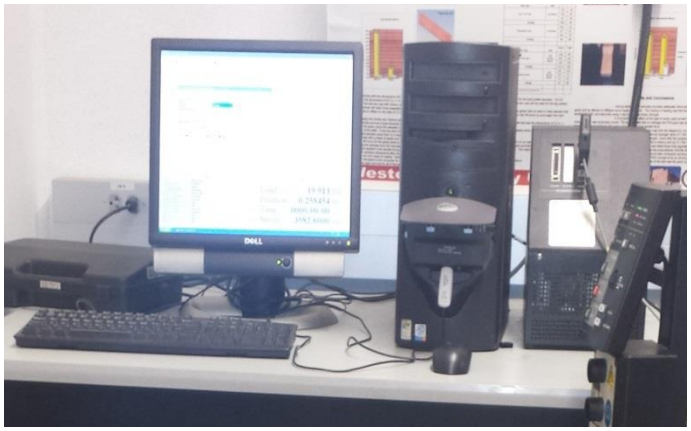

Figure 3: Computer running Partner Software

2.2.4 Imaging

The Large Chamber Scanning Electron Microscope (LC-SEM) was used to image all stainless steel dog bones. The large chamber scanning electron microscope is located at the Western Kentucky University Nondestructive Analysis Center (WKU NOVA Center). The LC-SEM is a one of a kind instrument; it has all of the features of a conventional SEM but it can study extremely large samples, allowing nondestructive investigation of components to be performed. The maximum sample size is 1.5m in diameter and a maximum sample weight of 650 lbs. The LC-SEM has a magnification up to 100,000x (<10nm resolution). The LC-SEM has the ability to move both the sample and the column, whereas a conventional SEM only moves the sample. The LC-SEM is capable of investigating samples using an *in-situ* uniaxial load frame. During a tensile test, the maximum axial force capacity is 90 kN. The LC-SEM comes equipped with a suite of instrumentation that includes: high-resolution imaging such as Secondary Electron Imaging (SE) for topographic imaging and Back-Scattered Electrons (BSE) for elemental contrast imaging, surface characterization such as Energy Dispersive Spectroscopy (EDS) for chemical analysis and Fourier Transform-Infrared (FT-IR) spectroscopy for materials identification, corrosion, failure, quality control analysis, metal microstructure such as Electron Backscatter Diffraction (EBSD) for crystallography and Focused Ion Beam (FIB) for ion milling for subsurface examination. (6)

The SE and EDS features of the LC-SEM were used to investigate type 304 and 316 stainless steel dogbone samples. The microscope works by accelerating electrons carrying significant amounts of kinetic energy as this energy is dissipated a variety of

signals are produced by electron-sample interaction. (7) The electron beam is scanned across a stainless steel's surface. Electrons interact with the stainless steel and are identified by specific detectors to obtain a variety of information. As well, the generation of x-rays due to the interaction of the electron with the sample is used for elemental composition information. In this investigation, secondary electrons (SE) and energy dispersive x-ray spectroscopy (EDS) were used for imaging and elementary composition, respectively. Secondary electrons are emitted from the atoms occupying the top surface of the stainless steel after interacting with the electrons from the LC-SEM. On detection a high-resolution image of the sample can be displayed. Interaction of the electrons from the SEM interacts with the electrons within atoms in the stainless steel. Electron ejected from an inner shell after interaction with an SEM electron can occur. After a time, an electron transition of an upper shell to an inner shall occurs with the emission of an x-ray that that is characteristic of element from which is originated. (18) When used in "spot" mode, we typically were able to collect a full elemental spectrum within several minutes. Supporting software makes it possible to identify peaks in the spectrum to identify the elements and also to calculate abundances. (8)

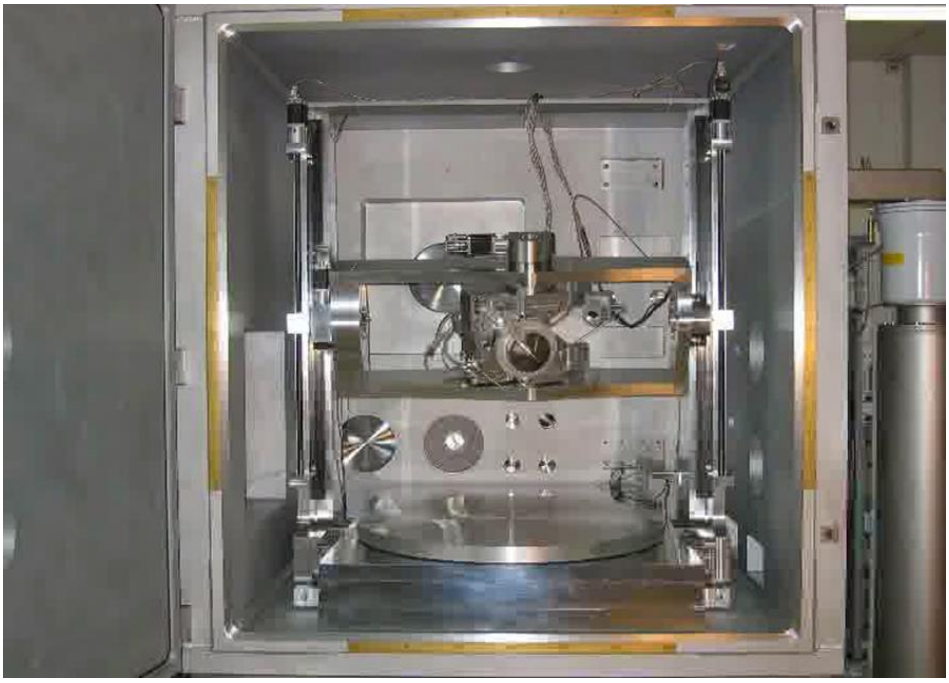

Figure 4: Large Chamber Scanning Electron Microscope

Section 2.3 Procedure

2.3.1 Preparation

Two- 0.20" x 6" x 50" stainless steel sheets were order from McMaster Carr for the fabrication of the stainless steel flat bars with reduced-section also known as dog bone specimens. The stainless steel sheets were cut into 3.511 x 0.750 inches stainless steel dog bone specimen using water jet cutter. All water jet cutting was done Big Blue Saw. A water jet cutter is a tool capable of slicing into metal or other materials using a jet of water at high velocity and pressure, or a mixture of water and an abrasive substance.(9)

a.)  b.)  c.) 

Figures 5 a-c: Stainless Steel Dogbone

2.3.2 Polishing

A set of 304 and a set of 316 stainless steel dog bones were polished using a LECO AP-60. Throughout this thesis, the term "set" will be used to quantify five stainless steel dog bones. First, the sets were polished for one minute each on 180 grit silicon carbide grinding paper, 320 grit silicon carbide grinding paper, and 600 grit silicon carbide grinding paper. Silicon carbide is a common abrasive that has been used for years because of its effectiveness and reliability for grinding metallic metallographic specimens. (10) Silicon carbide grinding papers are assigned grit sizes; the grit size correlates to the desired particle size (in micron) of the substance being grinded. Lower numbers have coarser grits i.e. larger size particles and larger numbers such as have finer grits i.e. smaller size particles. (11) The table below shows how grit size and micron compare.

Grit	Microns	Grit	Microns
1000 (fine)	7 (small)	90	145
900	9	80	165
800	12	70	203
600	16	60	254
320	31	54	305
700	32	46	356
280	39	36	483
500	40	30	559
400	45	24	686
240	50	20	940
220	63	16	1,092
180	76	14	1,346
150	89	12	1,600
120	102	10	1,854
100	122	8(coarse)	2,210(large)

Table 1: Grit and Micron Sizes (11)

Next, six-micron diamond compound paste and polish extender were used to polish the sets for three minutes on ultra-fine silk cloth. A dime size amount of six-micron diamond compound paste was placed on the side to be polished on each stainless steel dog bone and the ultra-fine silk cloth. Then, ten millimeter of polish extender was poured one the ultra-fine silk cloth. Diamond compound paste is an oil soluble paste used as to remove the grit scratches from stainless steel. (10)The polish extender is an alcohol-based liquid that aids in improved material removal. (12) Six-micron diamond compound paste is used because of its ability to remove 400-grit scratches. (10) The ultra- fine silk cloth is a woven, artificial silk polishing cloth consisting of a very thin layer of silk. (12)

Finally, one-micron diamond compound paste and polish extender were used to polish the sets for one minute on red felt cloth. A dime size amount of one-micron diamond compound paste was placed on the side to be polished on each stainless steel dog bone and the red felt cloth. Then, ten millimeter of polish extender was poured one the red felt cloth. One-micron diamond compound paste is used because of its ability to

remove 600-grit scratches. (10) Red felt cloth is a hard, durable cloth. (12) All polishing was done at 200 revolutions per minute. All equipment used for polishing was manufactured by LECO Corporation.

2.3.3 Tensile Testing

Using Instron and Partners software, tensile testing was conducted on polished sets of 304 and 316 stainless steel and unpolished sets of 304 and 316 stainless steel dog bones; the unpolished sets were later polished before examination under scanning electron microscope. The Instron applies tensile force (a force applied in opposite directions) on the stainless steel dog bones, and then measures the force and elongation. The force was created using the hydraulic cylinder of the Instron. The applied force needed for testing the sets of 304 and 316 was determined by the load at failure for one stainless steel dog bone of each set. The load at failure was divided to achieve four different points until failure. The remaining samples in each set of 304 and 316 were then tested at their designated pull point. Pull points are the maximum amount of load applied to the sample. The table below shows the designated five pull points tested for unpolished 304 stainless steel set.

Percent to Failure	Load(lbs)
21%	206
41%	407
61%	612
81%	815
100%	1004

Table 2 Test Points of Unpolished 304 Stainless Steel

Using the Partner software, the Instron was zeroed to ensure accurate data acquisition. Then, the dimensions of the dog bone and designated load for the dog bone were input into the Partner software program. The dog bone was placed into the grips designated for sheet specimen and the program began recording the induced stress. This procedure was repeated every stainless steel dog bone in each set.

2.3.4 Imaging

The sets of 304 and 316 stainless steel dog bones were imaged using a large chamber scanning electron microscope. The microscope focused on roughly the middle of the sample and points of facture while using secondary electrons to image the samples. The same magnification was used for each sample. At the points of facture, Energy Dispersive Spectroscopy (EDS) was used to collect element composition analysis.

RESULTS

Experimental results have yielded visual clues of the effects of stress on stainless steel and how this relates to the chemical composition of the nickel content of fractured dog bone. Stress bands, stress striations, microvoids, and microcracks were evident on the all dogbones tested. Stress bands are defined as raised vertical lines at least 5 micrometers in width. Below is an image of stainless steel dogbone with arrows pointing to example of a stress band.

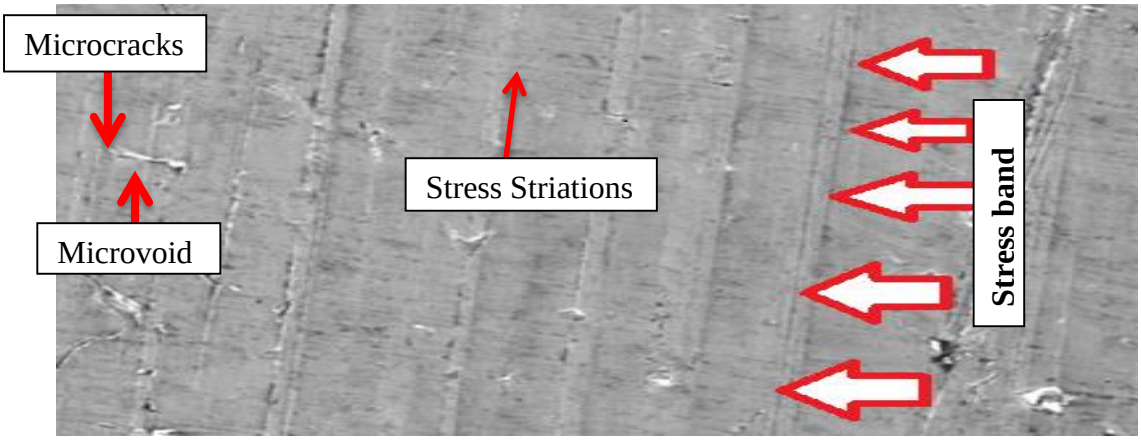

Figure 6: Example of Mirocracks, Mirovoids, and Stress bands

3.1 UNPOLISHED 304 STAINLESS STEEL

Five unpolished 304 stainless steel specimens were pulled at four different points as recorded in the table below and one dog bone was pulled until failure; then polished and imaged.

Percent to Failure	Load(Newton)
21%	916
41%	1810
61%	2722
81%	3625
100%	4466

Table 2: Test Points of Unpolished 304 Stainless Steel

The graph below shows the load elongation curve for a unpolished 304 stainless steel placed under tension until failure. The curve on the graph demonstrates the typical deformation phases of stainless steel during tensile test. The phases are elastic region, yield point, plastic region, and facture.

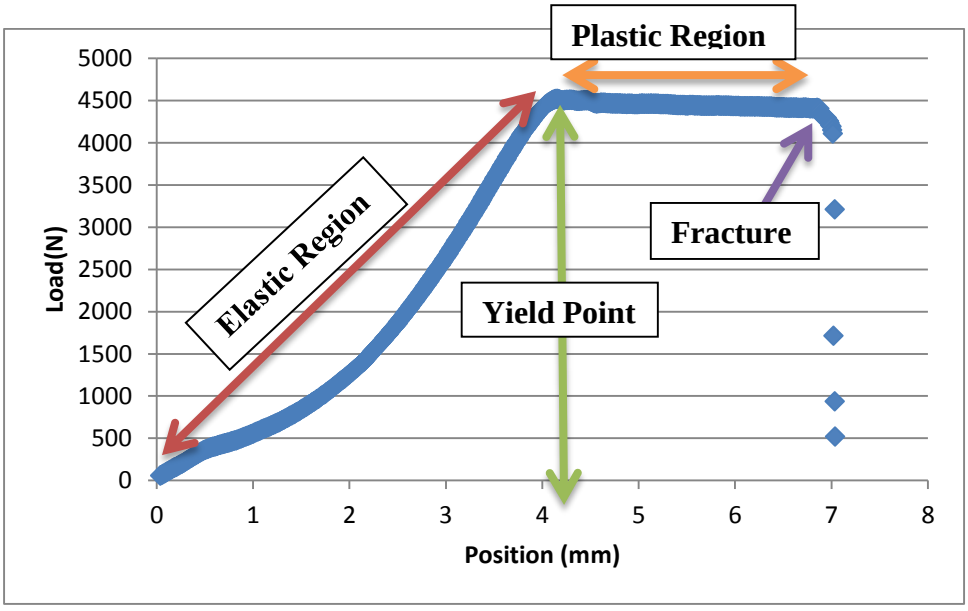

Figure 7: Unpolished 304 Stainless Steel

During the elastic region, deformation is causes by the amount of stress applied to the stainless steel that if the stress were removed the material would return to the dimension it had before the load was applied. Elastic deformation is reversible and therefore not permanent. However, while the physical dimensions remain unchanged surface structure is irreversibly altered. During the elastic region, stress bands, mirocracks and microvoids are present. The yield point is the minimum amount of stress needed for permanent deformation. Any value higher than the yield point is the plastic region. During the plastic region, there is a plateau where the stress increases under a constant load until the cross-sectional area of the stainless steel begins to decrease in a localized region of the specimen, instead of over its entire length. This leads to the facture of the stainless steel dogbone. (13) During the elastic region the dog bone is elongated 3.98 mm at 44392.81 N. During the plastic region the dog bone is elongated an additionally 3.06mm for a total displacement of 7.04 mm before facture.

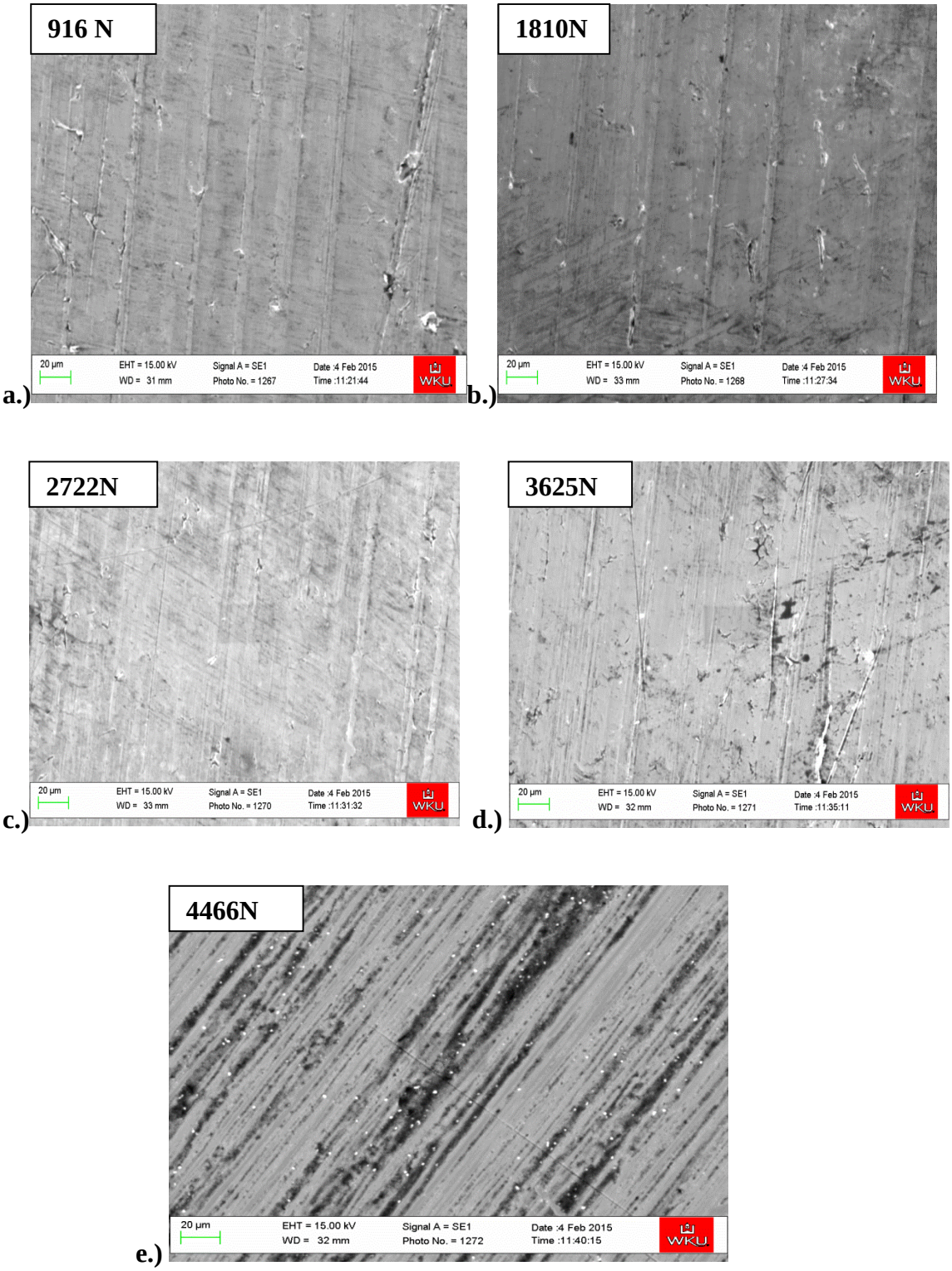

Figure 8 (a-e) :SEM IMAGES OF UNPOLISHED 304 STAINLESS STEEL Above are images of the stainless steel dog bones' surface after the test point load has been applied. a.) 916 N, b.) 1810N, c.) 2722N, d.)3625N , and e.)4466N

The images above are a surface progression of the induced stress until failure. In image a.), numerous stress band, microvoids, and microcracks are apparent. In image b.), only three definite stress bands are seen also microvoids and microcracks are apparent. In image c.), the definition of the stress bands start to diminish also microvoids and microcracks are apparent. In image d.), the definition of the stress bands have completely vanished but microvoids and microcracks are still apparent. In image e.), failure, no stress bands are seen but slanted stress striations have appeared.. EDS was used on the fractured dog bone to examine elemental differences between surface and crack compositions.

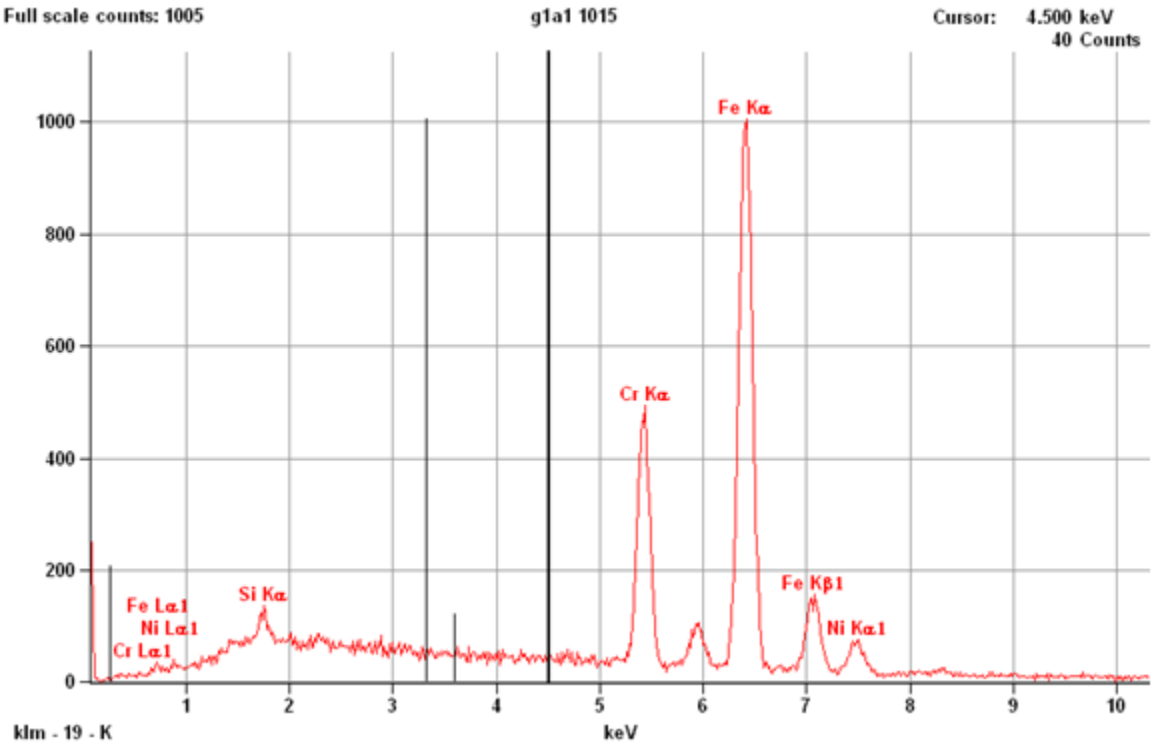

Figure 9: Surface Composition of Unpolished 304 Stainless Steel

Element	Atom %
Si	1.22
Cr	19.58
Fe	72.66
Ni	6.54
Total	100.00

Table 3: Surface Composition of Unpolished 304 Stainless Steel

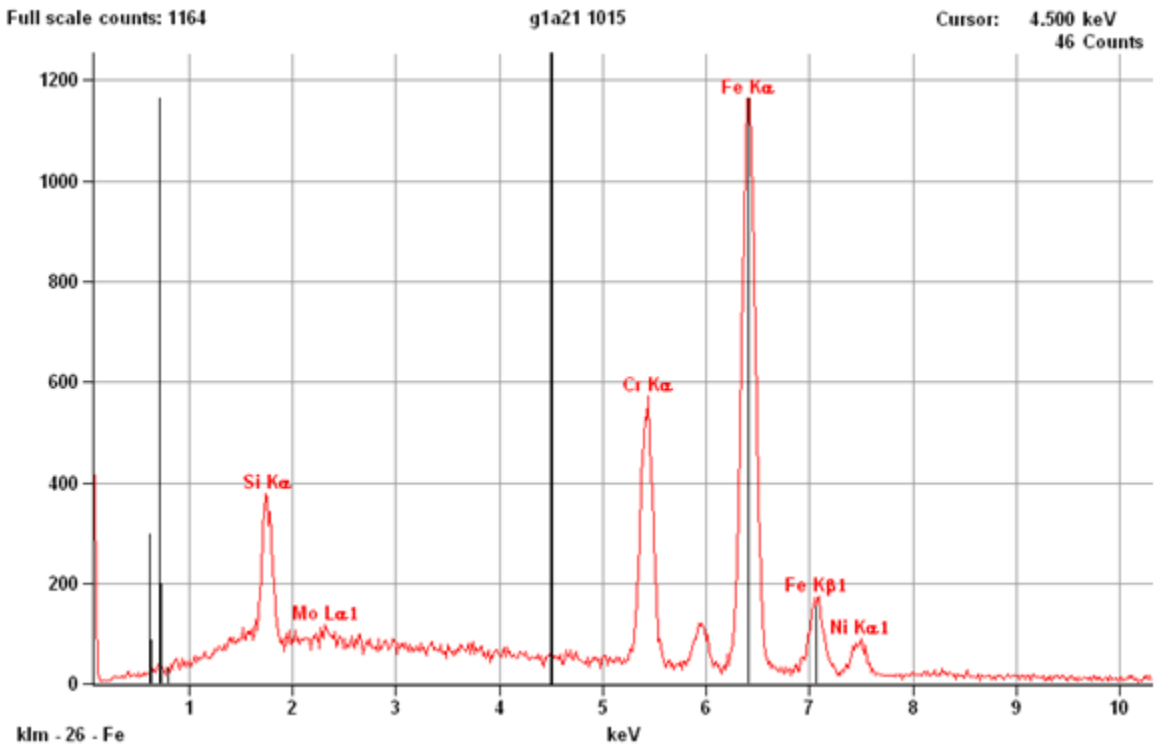

Figure 10: Crack Composition of Unpolished 304 Stainless Steel

Element	Atom %
Si	6.06
Cr	18.68
Fe	68.42
Ni	6.41
Mo	0.43
Total	100.00

Table 4: Crack Composition of Unpolished 304 Stainless Steel.

Comparing the nickel content in table 3 and 4 confirm there is .13% difference in nickel content in the crack versus the surface. The surface had .13% more nickel.

3.2 UNPOLISHED 316 STAINLESS STEEL

Five unpolished 304 stainless steel specimens were pulled at four different points as recorded in the table below and one dog bone was pulled until failure; then polished and imaged.

Percent to Failure	Load(Newton)
20%	436
40%	867
61%	1303
81%	1739
100%	2154

Table 5: Test Points of Unpolished 316 Stainless Steel

The graph below shows the load elongation curve for an unpolished 316 stainless steel placed under tension until failure.

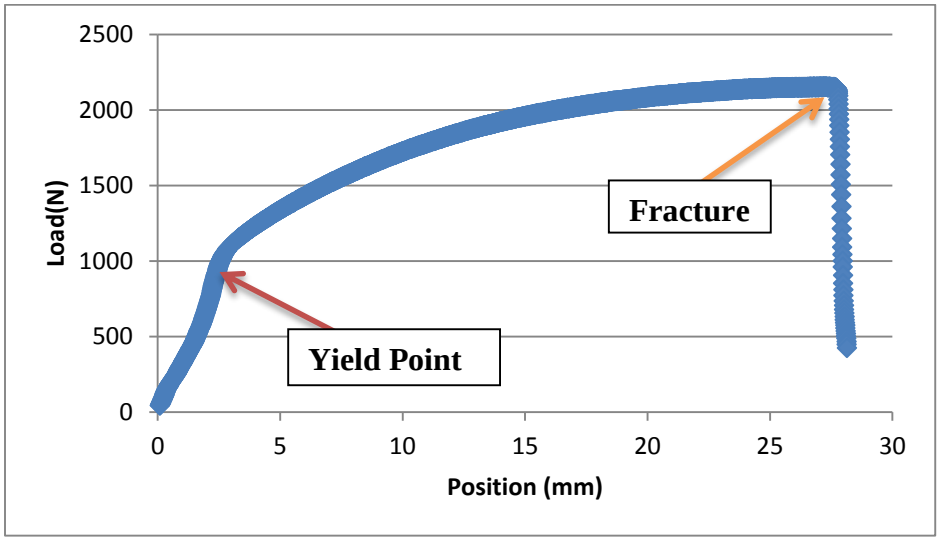

Figure 11: Unpolished 316 Stainless Steel

During the elastic region the dog bone is elongated 2.48 mm with a yield point at 967.66 N. During the plastic region the dog bone is elongated an additionally 24.99 mm before fracturing at 2154 N.

a.) 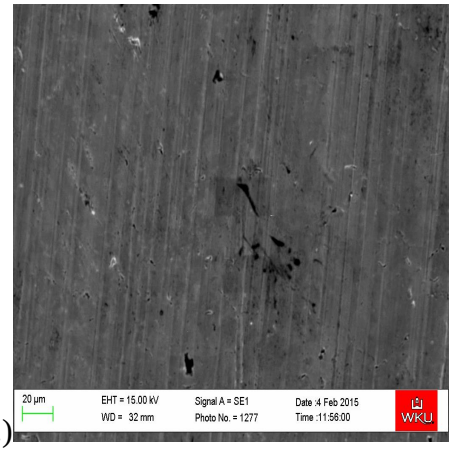

b.) 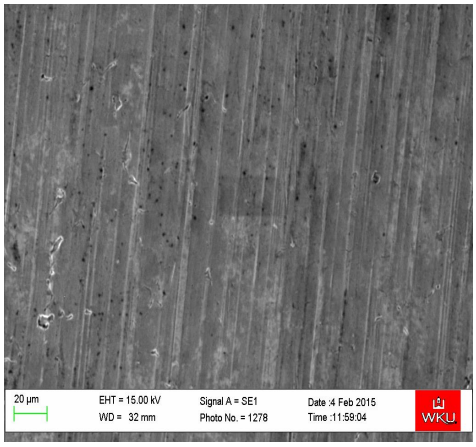

c.) 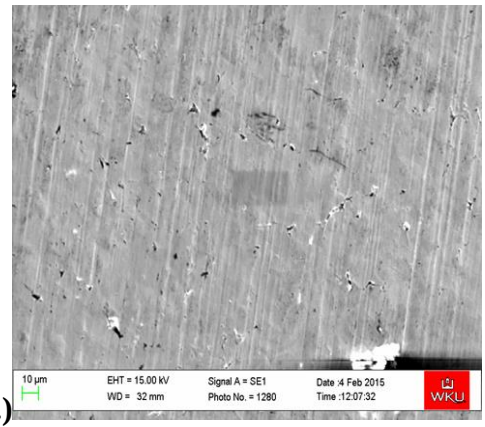

d.) 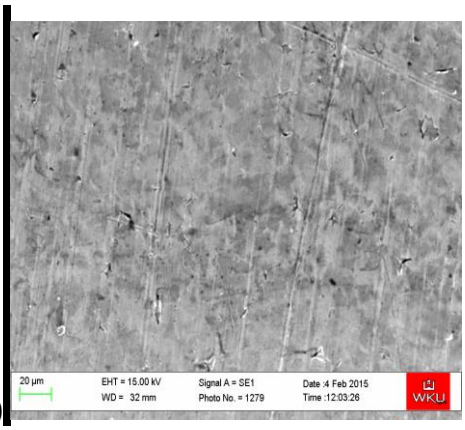

e.) 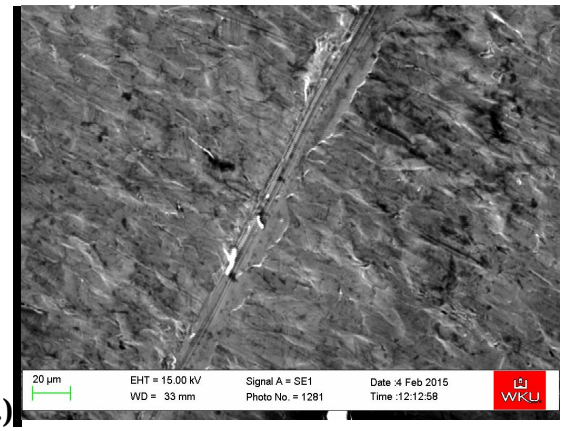

Figure 12 (a-e): SEM IMAGES OF UNPOLISHED 316 STAINLESS STEEL Above are images of the stainless steel dog bones' surface after the test point load has been applied a.) 436N, b.) 867N, c.) 1303N, d.) 1739N , and e.) 2153N

The images above are a surface progression of the induced stress until failure the 316 stainless steel. In image a.) through c.), numerous stress band, microcracks, and

microvoids are apparent. In image d.), the definition of the stress bands start to diminish. In image e.), failure, one prominent stress band is seen but slanted stress striations have appeared also microcracks and microvoids are still apparent. The EDS was used on the fractured dog bone to examine the differences of surface and crack composition.

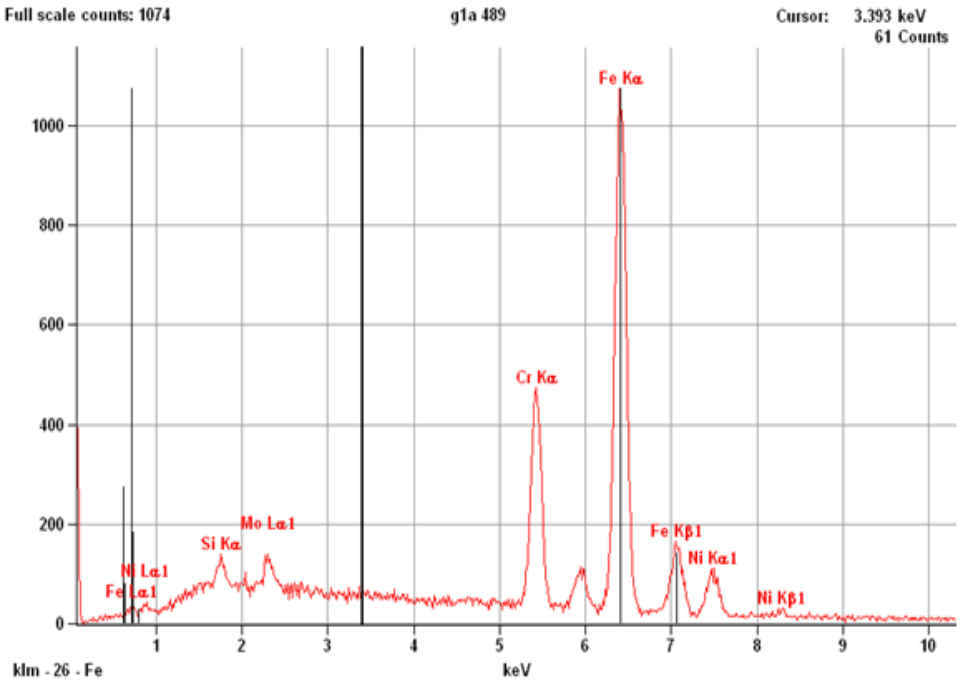

Figure 13: Surface Composition of Unpolished 316 Stainless Steel

Element	Atom %
Si	1.13
Cr	18.02
Fe	69.59
Ni	10.19
Mo	1.07
Total	100

Table 6: Surface Composition of Unpolished 316 Stainless Steel

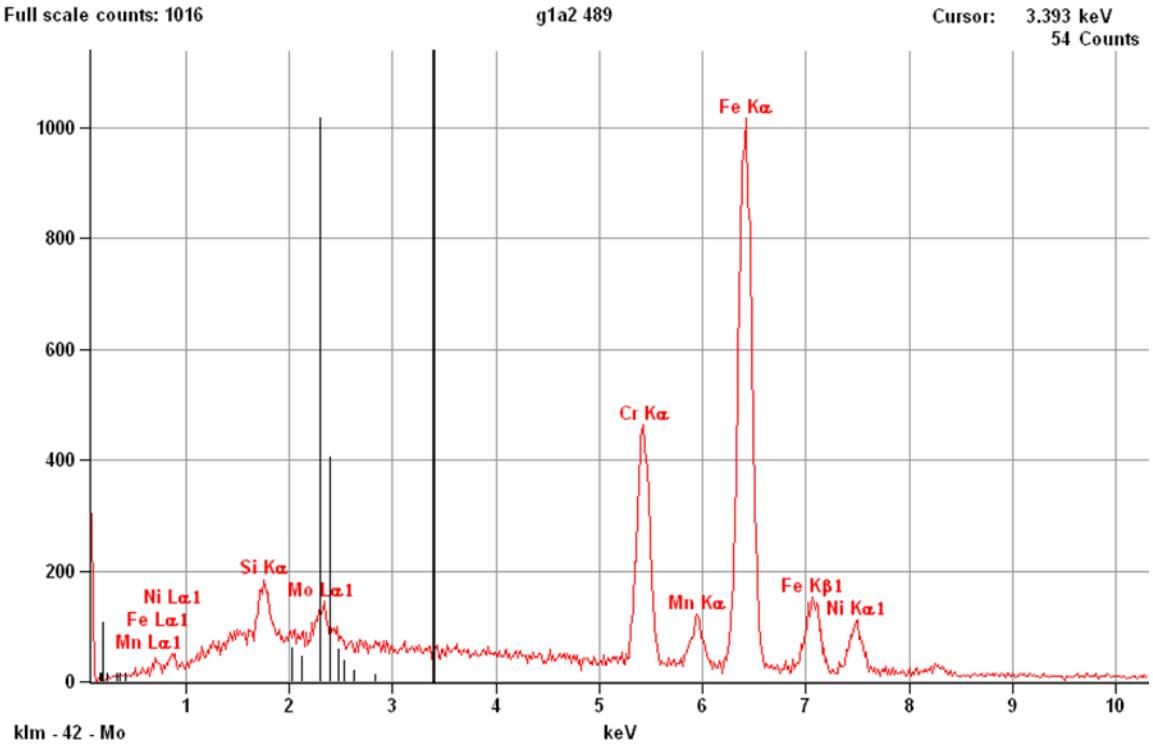

Figure 14: Crack Composition of Unpolished 316 Stainless Steel

Element	Atom %
Si	2.35
Cr	17.47
Mn	1.47
Fe	67.75
Ni	9.95
Mo	1.02
Total	100

Table 7: Crack Composition of Unpolished 316 Stainless Steel

Comparing the nickel content in table 6 and 7 confirm there is a .24% weight difference in nickel content between surface and the crack. The surface had .24% more nickel.

3.3 POLISHED 304 STAINLESS STEEL

Five polished 304 stainless steel specimens were pulled at four different points as recorded in the table below and one dog bone was pulled until failure; then the set was imaged

Percent to Failure	Load(Newton)
20%	916
40%	1810
61%	2722
81%	3625
100%	4502

Table 8: Test Points of Polished 304 Stainless Steel

The graph below shows the load elongation curve for a polished 304 stainless steel placed under tension until failure.

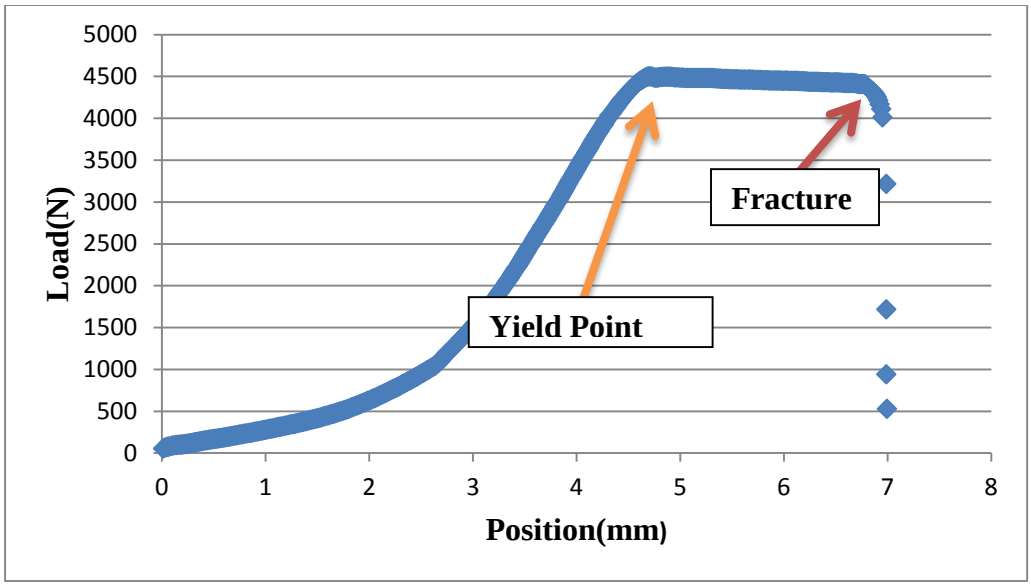

Figure 15: Polished 304 Stainless Steel

During the elastic region the dog bone is elongated 4.49 mm with a yield point at 4302 N. During the plastic region the dog bone is elongated an additionally 2.5 mm before fracturing at 4502N.

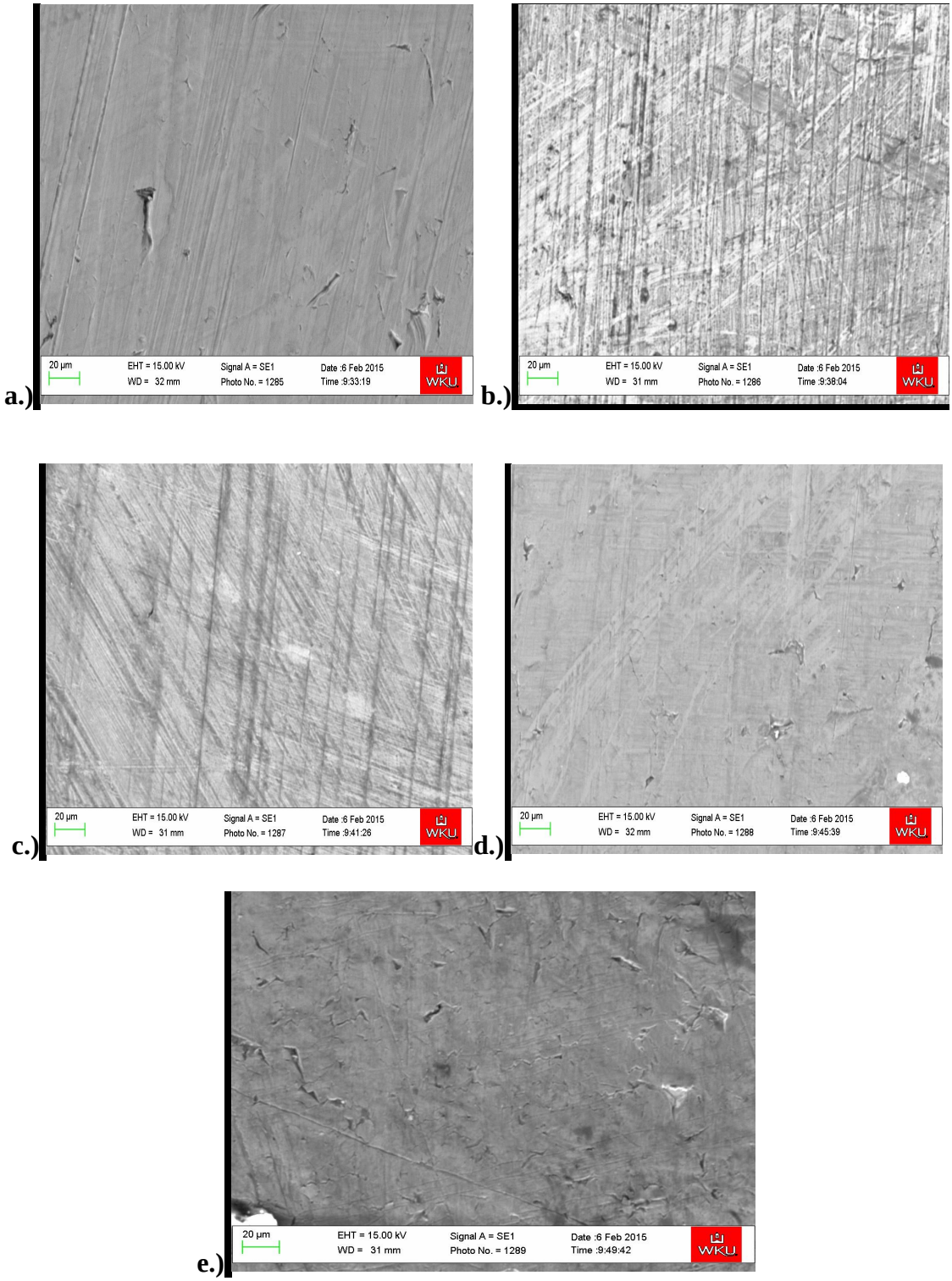

Figure 16 (a-e): SEM IMAGES OF POLISHED 304 STAINLESS STEEL Above are images of the stainless steel dog bones' surface after the test point load has been applied at variouis loads a.) 916 N b.)1810N c.) 2722N d.)3625N and e.)4502N

The images above are a surface progression of the induced stress until failure of the polished 304 stainless steel set. In image a.) through c.), numerous stress band, stress striations, microcracks and microvoids are present. In image d.), the definition of the stress bands start to diminish. In image e.), failure, the definition of the stress bands have completely vanished and few stress bands are seen. The EDS was used on the fractured dog bone to examine the differences of surface and crack composition.

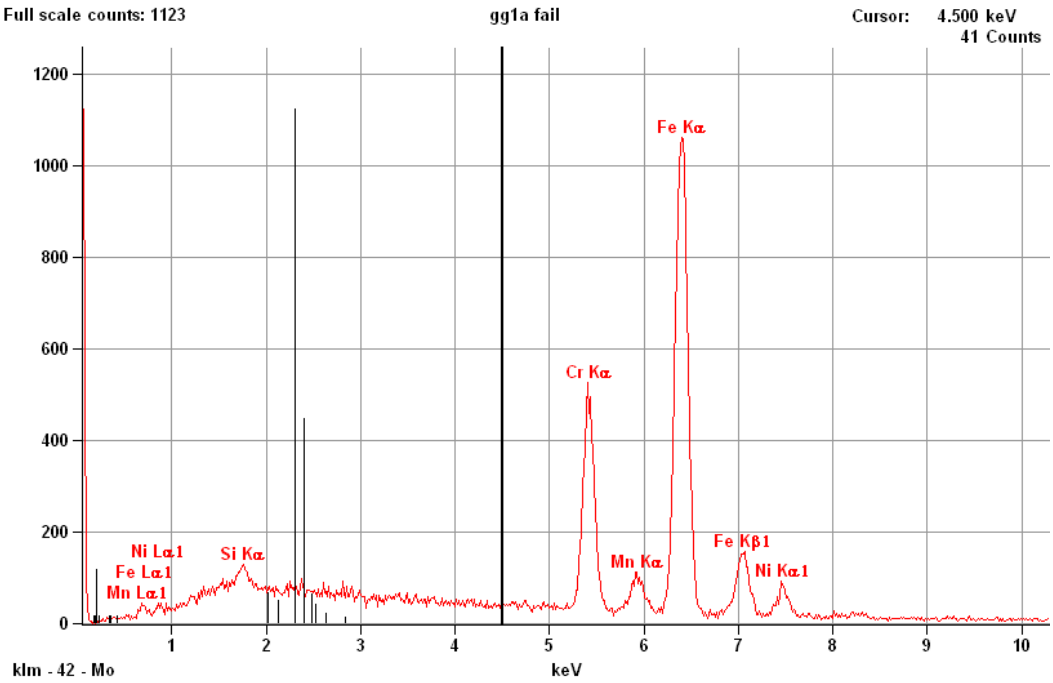

Figure 17: Surface Composition of Polished 304 Stainless Steel

Element	Atom %
Si	0.95
Cr	19.24
Mn	1.51
Fe	73.24
Ni	5.06
Total	100.00

Table 9: Surface Composition of Polished 304 Stainless Steel

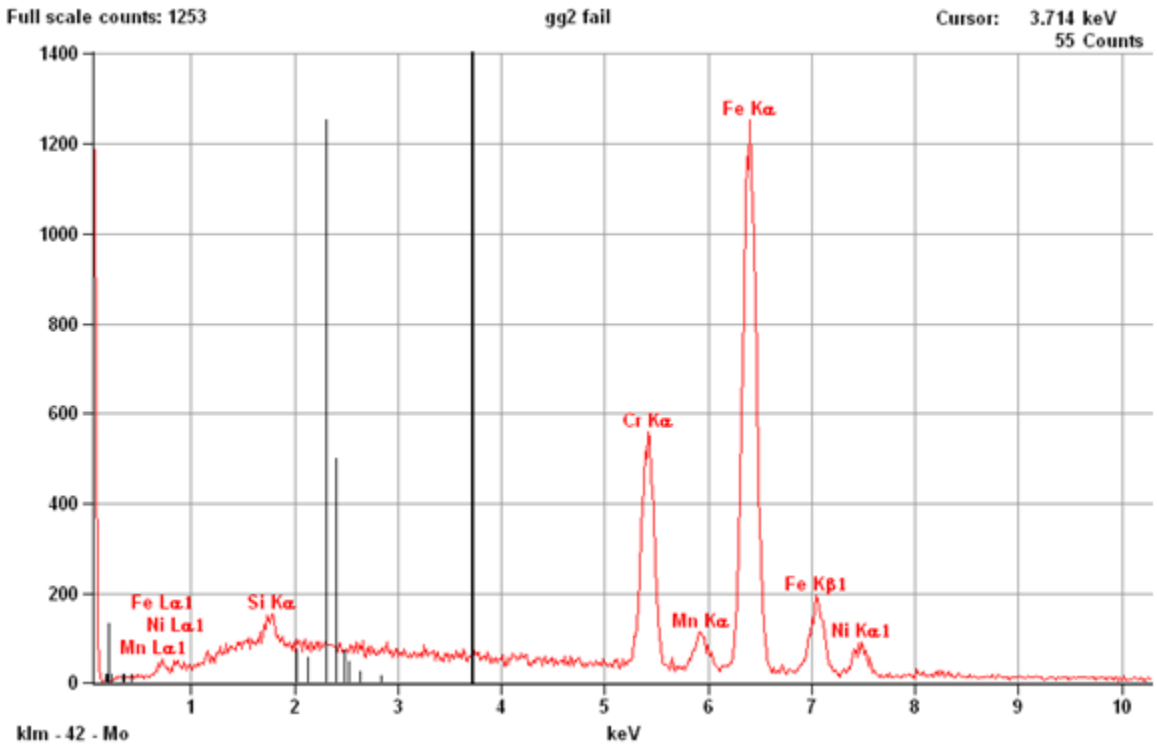

Figure 18: Crack Composition of Polished 304 Stainless Steel

Element	**Atom %**
Si	**1.42**
Cr	**18.49**
Mn	**1.26**
Fe	**73.00**
Ni	**5.83**
Total	**100.00**

Table 10: Crack Composition of Polished 304 Stainless Steel

Comparing the nickel content in table 9 and 10 show there is a .77% weight difference in nickel content in the crack versus the surface. The crack had .77% more nickel.

3.4 POLISHED 316 STAINLESS STEEL

Five polished 316 stainless steel specimens were pulled at four different points as recorded in the table below and one dog bone was pulled until failure; then the set was imaged.

Percent to Failure	Load(Newton)
20%	436
40%	867
60%	1303
80%	1739
100%	2175

Table 11: Test Points of Polished 316 Stainless Steel

The graph below shows the load elongation curve for a polished 316 stainless steel placed under tension until failure.

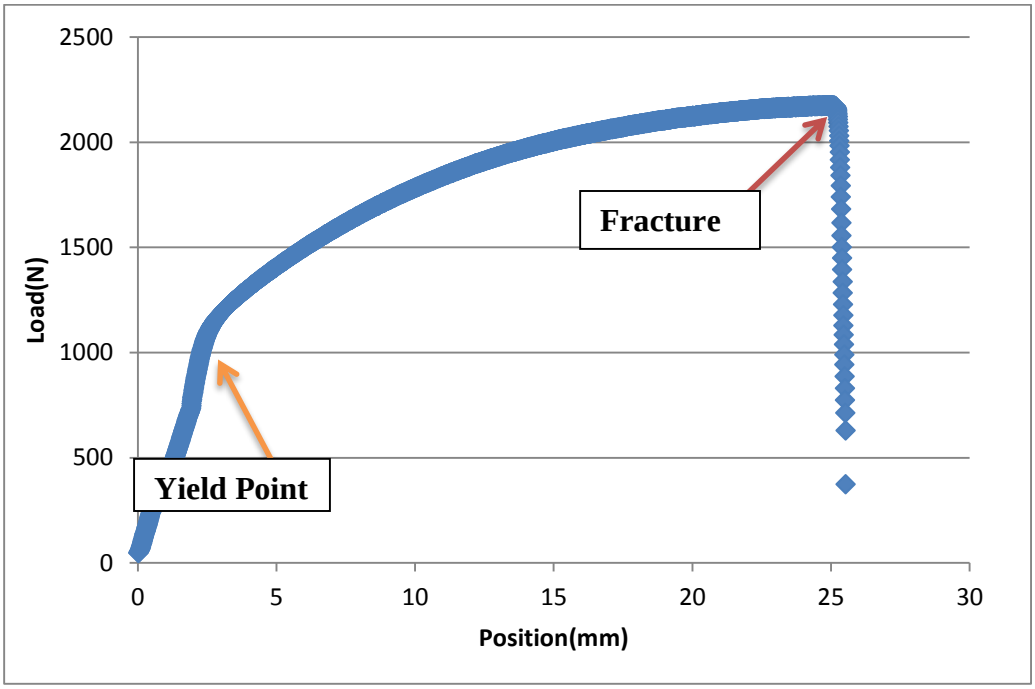

Figure 19: Polished 316 Stainless Steel

During the elastic region the dog bone is elongated 2.23 mm with a yield point at 967.83 N. During the plastic region the dog bone is elongated an additionally 22.8 mm before fracturing at 2175 N.

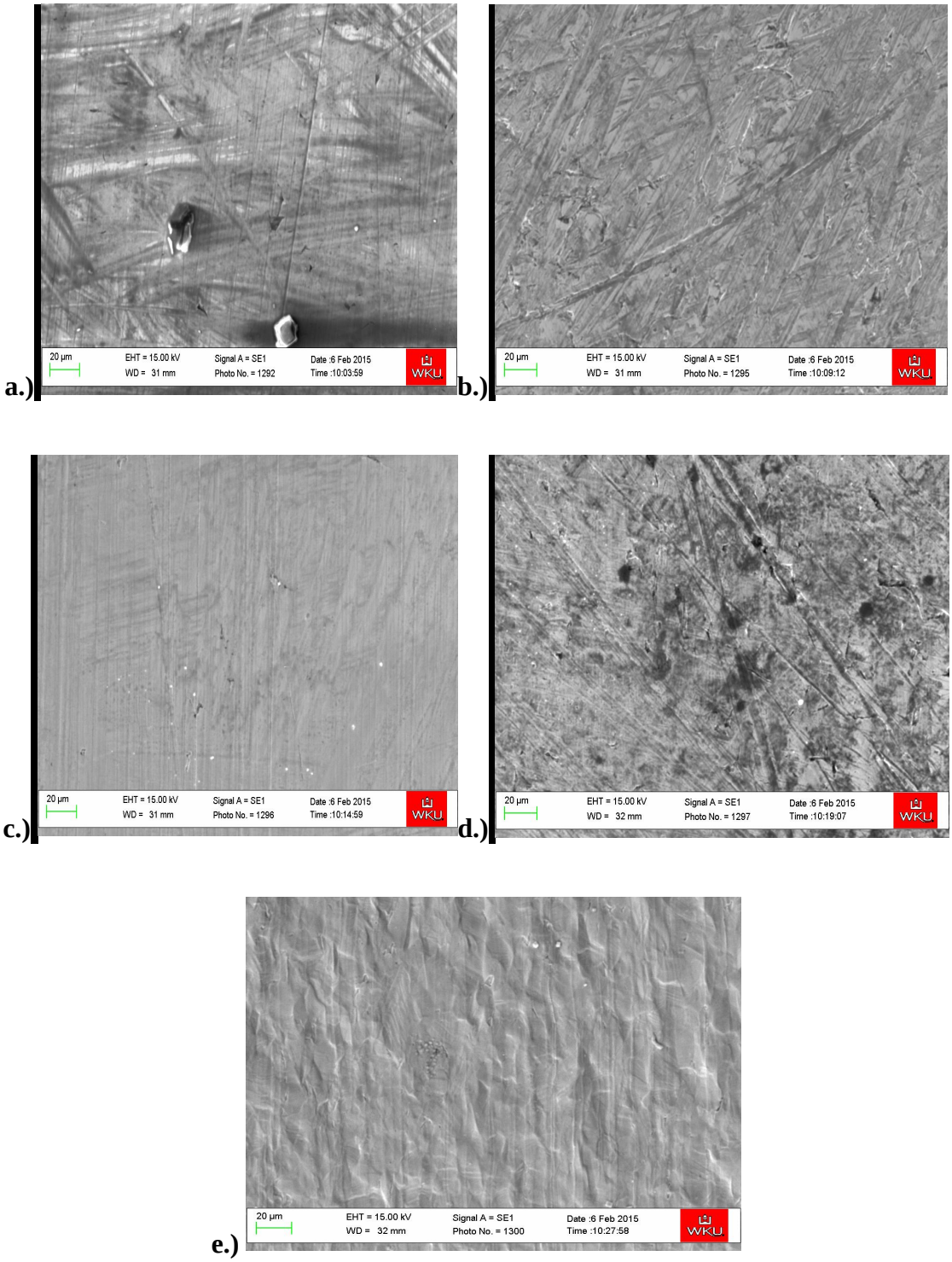

Figure 20 (a-e): SEM IMAGES OF POLISHED 316 STAINLESS STEEL Above are images of the stainless steel dog bones' surface after the test point load has been applied at various loads a.) 436N, b.) 867N, c.) 1303N, d.) 1739N, and e.) 2175N

The images above are a surface progression of the induced stress until failure of the polished 316 stainless steel set. In image a.) through e.), numerous stress band, stress striations, microcracks, and microvoids are apparent. The EDS was used on the fractured dog bone to examine the differences of surface and crack composition.

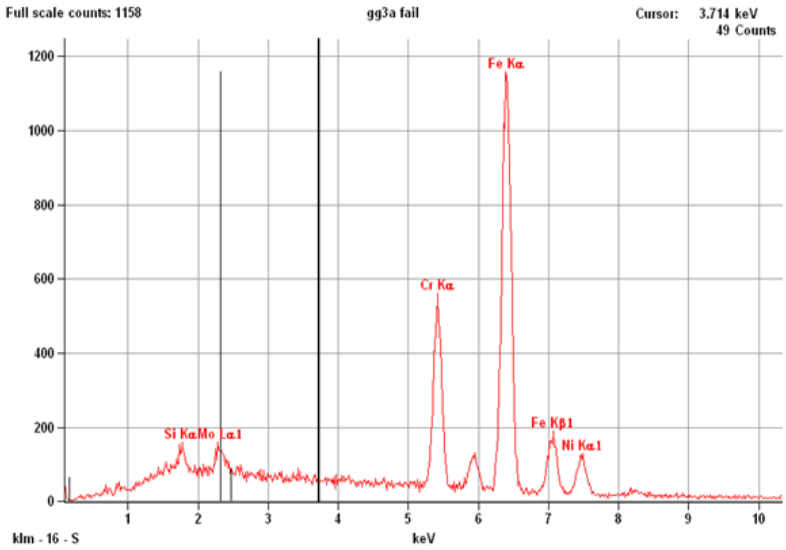

Figure 21: Crack Composition of Polished 316 Stainless Steel

Element	Atom %
Si	1.46
Cr	17.05
Mn	2.01
Fe	68.89
Ni	9.69
Mo	0.91
Total	100.00

Table 12: Crack Composition of Polished 316 Stainless Steel

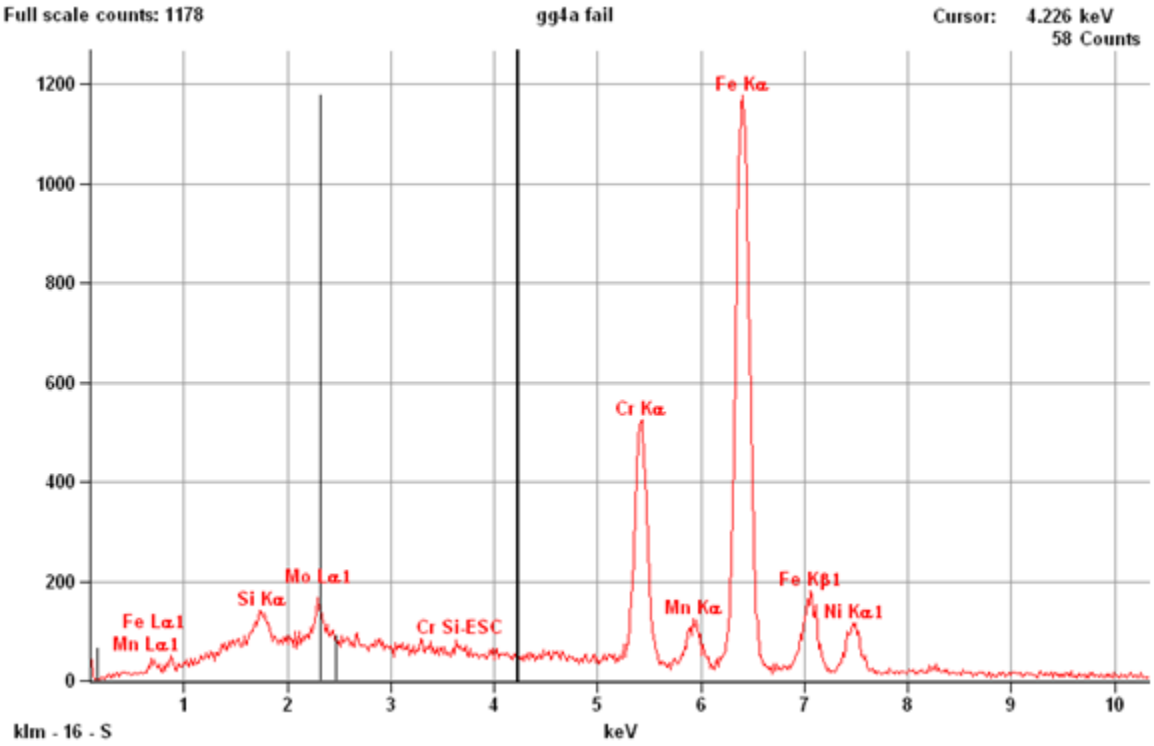

Figure 22: Surface Composition of Polished 316 Stainless Steel

Element	Atom
Si	1.12
Cr	18.28
Fe	70.52
Ni	10.07
Total	100.00

Table 13: Surface Composition of Polished 316 Stainless Steel

Comparing the nickel content in table 12 and 13 show there is a .38% weight difference in nickel content in the crack versus the surface. The crack had .38% more nickel.

DISCUSSION

The results of the experiment demonstrate the evolution surface morphologies of the polished and unpolished stainless steel dogbones. These results also show evidence of increased nickel content around the facture location of the polished dogbones. SEM images illustrate the evolution of the surface morphology at each pull point. The physical morphologies shown in the SEM images of the unpolished and polished stainless steel dogbones appear different; however, these differences are only due to imaging software and polishing technique. Overall the appearance of stress bands, stress striations, microvoids, and microcracks were evident on the all dogbones tested. Microvoids form in the area of stress; often microvoids nucleate and coalesce to form microcracks seen on the stainless steel dogbone. The induced stress on the stainless steel dogbone also causes "dimples". Dimples are microscopic cupules or concave depressions, these depressions stem from coalesce voids.(19) Stress bands and stress striations were most pronounced within the elastic region of each dogbone. This is evident when examining at Figure 8 a-b, Figure 9 a-c, Figure 10 b-c, and Figure 11 a, b, and d. Microvoids, and microcracks were most pronounced within the plastic region of each dogbone. This is evident when examining at Figure 8: d, Figure 9: c through d, Figure 10: d, and Figure 11: d. The stress bands and striations created during the elastic region are due to the bonds within the metal stretching and also contributed to beginning stages of martensitic transformation. The bonds start slipping or dislocating during the plastic region. The plastic region is where a martensitic transformation (i.e. solid-state diffusionless phase) takes place. This transformation is characterized by the formation of the shape of laths, (i.e. ruler shaped units, or plates). Deformation behavior of austenite stainless steel is

complex due to the microstructural transformations. Austenitic grades can undergo a transformation to martensite during plastic deformation at room temperature. This microstructural transformation from austenite to martensite has been shown to increase the formability. Formability is an evaluation of how much deformation a material can undergo before failure.(14-16) The polished and unpolished 304 stainless steel elongated an average of 7 mm before failure. The polished and unpolished 316 stainless steel elongated an average of 27 mm before failure.

In this thesis, it was hypothesized that more nickel content would be found near the facture points of the failed dogbones than on the surface of the dogbones. However, the nickel content of the unpolished stainless steel dogbones' factures had less nickel composition than the surface. Conversely, the nickel content of the polished stainless steel dogbones' factures had more nickel composition than the surface. The differences in nickel content for polished and unpolished at the facture points deem inconclusive results.

CONCLUSION

The knowledge of the fatigue behavior, deformation characteristics, and resulting microstructure after induced strain of type 304 and type 316 was investigated and discussed. The SEM images captured the surface changes during induced strain, which is important because this information creates opportunities for better understanding the capacities and applications of stainless steel. Unfortunately, the hypothesized increased nickel content theory gave inconclusive results. In order to produce conclusive results more sample stainless steel dog bone sets should be created and tested.

REFERENCES

1.) Sources of the Study of Harry Brearley and Stainless Steel: 4. Sheffield, United Kindom: Sheffield Libraries Archives and Inbformation, 2011

2.) "The History of Stainless Steel." 100 Years of Stainless Steel. International Stainless Steel Forum, n.d. Web.

3.) Segui, William T., and Cram 101. "Chapter 1: Introduction." E-Study Guide for Steel Design. N.p.: Contents Technologies, 2014. 11. Google. Web.

4.) Marquez, Derek. "Stainless Steel Grades." Portland Bolt Stainless Steel Grades Comments. Portland Bolt & Mfg. Co, 30 June 2010. Web.

5.) Boland, M.A., 2012, Nickel—Makes stainless steel strong: U.S. Geological Survey Fact Sheet 2012–3024, 2 p., available at http://pubs.usgs.gov/fs/2012/3024/

6.) "WKU Nondestructive Analysis (NOVA) Center." WKU Nondestructive Analysis (NOVA) Center. Western Kentucky University, 2010. Web. <http://largechamber.com/>.

7.) Swapp, Susan. "Scanning Electron Microscopy (SEM)." Geochemical Instrumentation and Analysis. National Science Foundation, n.d. Web. <http://serc.carleton.edu/research_education/geochemsheets/techniques/SEM.html>.

8.) Goodge, John. "Energy-Dispersive X-Ray Spectroscopy (EDS)." Energy-dispersive Detector (EDS). University of Minnesota-Duluth, 2012. Web. <http://serc.carleton.edu/research_education/geochemsheets/eds.html>.

9.) Arthur, Simon. "Waterjet Cutter: How It Works." Waterjet Cutter: How It Works. Instant Quote by Big Blue Saw. Big Blue Saw, n.d. Web. 05 Feb. 2015. https://www.bigbluesaw.com/faqs/parts/how-does-waterjet-cutting-work.html

10.)L. Dillinger, "Polishing," Met-Tips 13, Leco Corp., 1985

11.)Hueston, Frederick. M. (2007, 04). Polishing abrasives. Surface Fabrication, 13, 23-25. Retrieved from http://search.proquest.com/docview/274700841?accountid=15150

12.)LECO. Met Supplies Catalog. St. Joseph: LECO, 2014. LECO: Delivering the Right Results. LECO Corporation, 17 Sept. 2014. Web. http://www.leco.com/component/edocman/?task=document.viewdoc&id=1041 .

13.) Patnaik, Surya N., and Dale A. Hopkins. "Introduction: Stress-Strain Law."*Strength of Materials: A Unified Theory*. Amsterdam: Elsevier/Butterworth-Heinemann, 2004. 33-35. Print

14.) Hedstrom, Peter. *Deformation Induced Martensitic Transformation of Metastable Stainless Steel AISI 301*. Thesis. Luleå University of Technology, 2005. Sweden: Department of Applied Physics and Mechanical Engineering, 2005. Dec. 2005. Web.

15.) "What Is the Material Formability?" — *LS-DYNA Support*. N.p., 2015. Web.

16.) Yeddu, Hemantha K. *Martensitic Transformations in Steels – A 3D Phase-field Study*. Diss. KTH Industrial Engineering and Mangement, 2012. Stockholm: KTH Industrial Engineering and Mangement, 2012. KTH Industrial Engineering and Mangement, June 2012. Web

17.) "Elastic/Plastic Deformation." *Elastic/Plastic Deformation*. National Science Foundation, 2014. Web. <https://www.nde-ed.org/EducationResources/CommunityCollege/Materials/Structure/deformation.htm>.

18.) "SEM/EDS - Scanning Electron Microscopy with X-ray Microanalysis." University of Buffalo The State University of New York. Buffalo University, n.d. Web. <http://wings.buffalo.edu/faculty/research/scic/sem-eds.html>.

19.) Liu, A. F. "Deformation and Fracture Mechanism and Static Strength of Metal." *Mechanics and Mechanisms of Fracture: An Introduction*. Materials Park, OH: ASM International, 2005. 62-76. *Google*. Web.